Variable-angle internal-reflection Raman spectroscopy for depth-resolved vibrational characterization of polymer thin films

N. H. Fontaine and T. E. Furtak
Department of Physics, Colorado School of Mines, Golden, Colorado, 80401
(Received 26 September 1997)

We have developed a general technique that is capable of providing molecular signatures as a function of depth in a multilayer thin film. Variable-angle internal-reflection Raman spectroscopy has been used to locate buried interfaces with nanometer-scale precision and to determine refractive indices to within ± 0.0001. We have demonstrated this method in several applications, including the detection of toluene diffusion across a polystyrene/poly(methyl methacrylate) interface. [S0163-1829(98)06307-3]

Depth-resolved measurement of the molecular structure of thin polymer films can provide insight about diffusion and interface formation. Although techniques with this capability are available, they either require special facilities (neutron reflectivity) or are inherently destructive (secondary-ion mass spectrometry and other ion milling methods). By contrast, optical radiation has the potential to provide depth-dependent information without disturbing the sensitive conditions that frequently exist in these systems. In particular, variable-angle internal-reflection Raman spectroscopy (VAIRRS) is well suited to the task of measuring the distribution of molecular concentrations and orientations. However, until now, quantitative depth profiling using an internal reflection approach has not advanced beyond the demonstration phase.[1,2]

We report here the completion of several essential steps toward developing VAIRRS into a reliable depth-profiling technique. We have identified and quantified precision and accuracy limits as well as common systematic errors. The details of our methodology are presented elsewhere.[3] In this paper, we outline the essentials of our approach, and present a summary of demonstration experiments that show how to extract the depth dependence of a Raman signature. Our objective has been to study a sample containing a fabricated discontinuity. We sought to show that VAIRRS was capable of locating the discontinuity and therefore of yielding a crude depth profile under those conditions. Beyond that, however, our method has also identified the migration of a small molecule (toluene) across the discontinuity.

A representation of the experiment appears in Fig. 1.

The incident medium is an internal reflection element (IRE) made of sapphire. Its refractive index is larger than that of the sample, which extends from $z=0$ to $z=d$. The scattered light is collected from the air side of the sample with an optical fiber, as shown. Raman scattering that originates at a particular depth, z, within a differential thickness δz contributes to a differential detected intensity $\delta I(\theta,z|\overline{\nu})$, which is proportional to the local Raman source function $C(z|\overline{\nu})$, and the local optical energy density $|E(\theta,z)|^2$, according to

$$\delta I(\theta,z|\overline{\nu}) \propto C(z|\overline{\nu})|E(\theta,z)|^2 \delta z. \tag{1}$$

We note that θ is the angle of incidence (defined within the IRE) at the IRE/polymer interface, and that $\overline{\nu}$ is the Stokes wave number of the center of a particular feature in the Raman spectrum whose integral magnitude is δI. By concentrating on a restricted region of the Raman spectrum, within a range around $\overline{\nu}$, one can tailor a VAIRRS experiment to provide information about specific molecular identities, orientations, and other characteristics of the sample to which the Raman effect is sensitive.

The measured signal includes contributions from the entire sample, at all values of z.

$$I(\theta|\overline{\nu}) = \int \delta I(\theta,z|\overline{\nu}). \tag{2}$$

The goal of the VAIRRS experiment is to extract $C(z|\overline{\nu})$ from high precision measurement of the θ dependence of $I(\theta|\overline{\nu})$. This is accomplished by modeling $I(\theta|\overline{\nu})$ using $C(z|\overline{\nu})$ as an adjustable function. The optical field $E(\theta,z)$ can, in principle, be calculated.[4] However, this depends on the refractive index $n(z')$ throughout the sample, not just at z. In general, $n(z')$ and $C(z'|\overline{\nu})$ are coupled, since both are derived from the local molecular structure.[5]

To make the modeling tractable it is practical to divide the film into a small number of layers. This is illustrated in Fig. 1, where layer i, with thickness $h(i)$, is one of $N-2$ layers, and part of the overall system of N media. In this simplification, each layer is assumed to be homogeneous, with re-

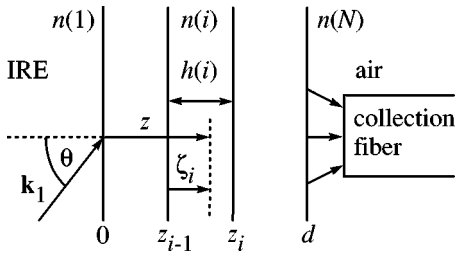

FIG. 1. Schematic arrangement for the VAIRRS experiment. The sample extends from $z=0$ to $z=d$, and is bounded by the internal reflection element (IRE) and air. The angle of incidence θ is reported within the IRE. A fiber optic bundle was used to collect the Raman scattered light.

gard to both $C(\zeta_i|\overline{\nu}) \equiv C(i|\overline{\nu})$ and $n(\zeta_i) \equiv n(i)$. The total optical energy within layer i is proportional to

$$\mathcal{E}(\theta,i) \equiv \int_0^{h(i)} |E(\theta,\zeta_i)|^2 d\zeta_i . \tag{3}$$

The detected intensity can then be approximated by a sum over layers:

$$I(\theta|\overline{\nu}) = \alpha \sum_{j=2}^{N-1} C(j|\overline{\nu}) \mathcal{E}(\theta,j) + \beta(\overline{\nu}). \tag{4}$$

The constant α is the product of scale factors such as the amplitude of the incident field and the efficiency of the detection system. The constant β accounts for angle-independent sources of background, such as scattering from the IRE.

The problem of depth profiling reduces to that of determining the relative magnitudes of the coefficients $C(j|\overline{\nu})$ that enable Eq. (4) to most closely reproduce the experiment. The analysis hinges on careful, self-consistent modeling of the optical fields in each layer. Total internal reflection from the jth interface occurs if the incident angle (in medium 1) exceeds the critical angle, $\theta_{c,j} = \arcsin[n(j+1)/n(1)]$. The z component of the wave vector in medium j, $k_z(\theta,j) = (2\pi/\lambda)\{[n(j)]^2 - [n(1)\sin\theta]^2\}^{1/2}$, is real positive for $\theta \leqslant \theta_{c,j}$ and imaginary positive for $\theta \geqslant \theta_{c,j}$. It is important to avoid computation-related errors that develop near the critical angles of the system. We have developed a numerical algorithm that is particularly robust, and which preserves the level of precision that is required to achieve meaningful fits of the model to the data.[3]

We present the results of two experiments designed to demonstrate the sensitivity of VAIRRS, and its ability to reveal depth-resolved information about a polymer system. All film layers were spun cast at 2000 rpm from a static dispense. In the first example a single-layer thin film of 250 000 m.w. atactic polystyrene (PS) was cast onto the IRE from a 9.0% toluene solution (by weight). This film was dried in air at 65°C for 75 min then measured with the VAIRRS method. This simple system ($N=3$) offers a baseline test of the precision of the method. In the second example ($N=4$) we established a well-defined buried interface between two immiscible polymers, PS and poly(methyl methacrylate) (PMMA).[8] Layer $j=2$ was 250 000 m.w. PS cast from an 8.6% toluene solution. The PS layer was dried at 80 °C in air for 52 h. Layer $j=3$ was cast directly onto the PS layer from 960 000 m.w. PMMA in 8.3% acetone solution. The bilayer was dried at 80°C for 14 h, prior to its study with VAIRRS.

The details of our experimental procedure are explained elsewhere.[3] We have been particularly careful to ensure that the incident beam interacted with the sample only once, and that the wave fronts were as close as possible to planar. The incident radiation was supplied by an argon-ion laser (TEM_{00}) operating at 514.52 ($\pm \approx 0.02$) nm. The angular uncertainty of $\approx 0.0068°$ was determined by the divergence of the incident beam as well as the collection optics of the fiber bundle. The sample was located 3.9 m from the waist of the beam to take advantage of the far-field character of the Gaussian wave front. The incident radiation was TE polarized, perpendicular to the c axis of the single-crystal sapphire IRE. The entrance and exit faces of the IRE were designed to minimize backreflection. The refractive index of the sapphire IRE $n_1 = 1.773\,90 \pm 0.000\,05$ (Ref. 6) (measured) and air $n_N = 1.000\,23 \pm 0.000\,02$ (Ref. 7) were treated as exactly known constants. The spectral ranges for the bands that serve to isolate information about the different materials in our experiment are shown in Fig. 2.

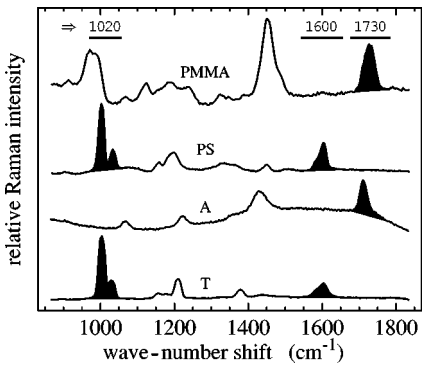

FIG. 2. Raman spectra of poly(methyl methacrylate) (PMMA), polystyrene (PS), acetone (A), and toluene (T). The integration ranges that identify $\overline{\nu} = 1020\ \mathrm{cm}^{-1}$, $1600\ \mathrm{cm}^{-1}$, and $1730\ \mathrm{cm}^{-1}$ are shown. To selectively probe PMMA and acetone, for example, the $\overline{\nu} = 1730\ \mathrm{cm}^{-1}$ band would be used to calculate $I(\theta|1600)$.

The results showing $I(\theta|1020)$ in the demonstration experiment with the single PS film are displayed in Fig. 3. The solid line is the model, using Eq. (4) in the form $I(\theta|1020) = \alpha\mathcal{E}(\theta,2) + \beta$. That is, with a single layer ($j=2$), assumed to be homogeneous, with $C(2|1020)$ set equal to unity. The parameters $n(2)$ and $h(2)$ were determined by iterative least-squares regression for the constants α and β over the three-dimensional reduced chi-square error space $\{n(2), h(2), \chi^2\}$. The values $n(2) = 1.5969 \pm 0.0001$, and $h(2) = 1197 \pm 5$ nm provided the best fit. The uncertainties were assigned by independent adjustments of $n(2)$ and $h(2)$ that yielded a 10% increase in the reduced chi-square above its minimal value.

To understand the details of the VAIRRS result consider the graphs of $|E(\theta,z)|^2$ which appear in Fig. 4. For each incident angle, the Raman intensity is proportional to

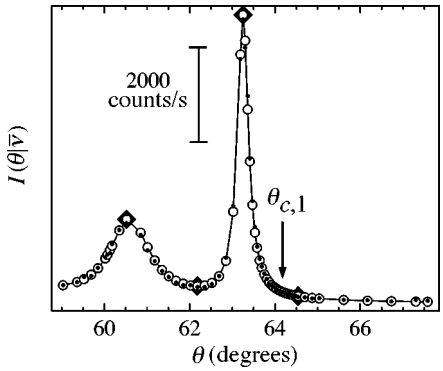

FIG. 3. Single-layer film: VAIRRS of the 1020-cm^{-1} band. Experiment (dots); theory (connected, open circles); critical angle ($\theta_{c,1}$) (arrow). Special angles (a)–(d) (identified by background, solid diamonds) refer to calculated energy density distributions in Fig. 4.

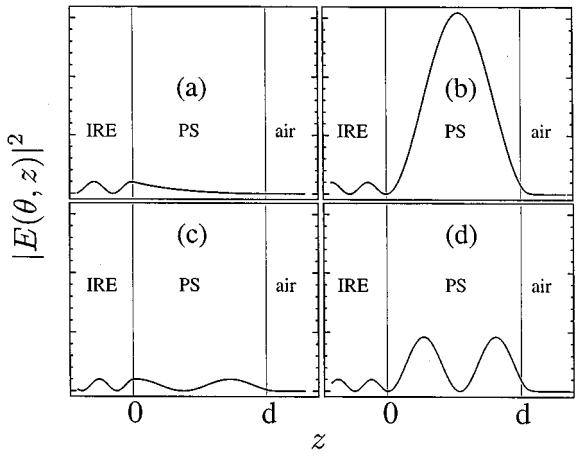

FIG. 4. Calculated optical energy densities for incident angles identified in Fig. 3: (a) in the evanescent regime $\theta > \theta_{c,1}$, (b) at the $m=1$ waveguide mode, (c) at the minimum, between $m=1$ and $m=2$, (d) at the $m=2$ waveguide mode.

$\mathcal{E}(\theta,2)$, which is the area under the curve within the limits of the polymer. As θ changes, the film is sampled with different distributions of the incident optical energy. A model for the spatial dependence of the source function [a constant in this case, but, in general, associated with the set of $C(j|\overline{\nu})$] must reproduce the data for *all* values of θ and, therefore, for all values of j (or z).

The maxima in Fig. 3 correspond to waveguide conditions within the film at θ satisfying $2h(2)k_z(\theta,2)+\pi+2\arctan[-ik_z(\theta,3)/k_z(\theta,2)]=2\pi m$, where m is the order of the mode.[9,10] With the refractive indices $n(1)>n(2)>n(3)$, these modes are radiative (leaky) at the PS/sapphire interface. However, it is clear that constructive interference still leads to substantial optical energy enhancement. This mechanism is exploited in the already established ''waveguide Raman'' technique, which uses thin-film samples that are optically *isolated*.[11] In that type of experiment the optical field distributions are limited to those that are associated with the propagating modes and are not continuously variable, as in our version of VAIRRS.

The modeling procedure involves adjustment of $n(2)$ and $h(2)$. These can be independently established, even though they are coupled in determining the optical path length within the film. The independence is related to the phase change at the $j=2/j=3$ boundary, which is particularly sensitive to $n(2)$. As $n(2)$ increases, the entire pattern of modes in Fig. 3 shifts toward larger angles. By contrast, as $h(2)$ decreases, the angular separation between the resonant modes increases. More subtle changes created by varying either $n(2)$ or $h(2)$ can be observed at all values of θ. The parameters associated with the best fit are, therefore, unique.

The high quality of the fit between the experiment and the model is an indication that (a) the experimental procedure is reliable, (b) the plane-wave approximation is appropriate, provided the Gaussian beam is used in the far field limit, and (c) the PS film in this case was homogeneous.

The objective of the bilayer experiment was to test the ability of VAIRRS to quantitatively locate a buried interface between two different polymers, PS and PMMA. In this case resonant modes can be established in either of the two layers,

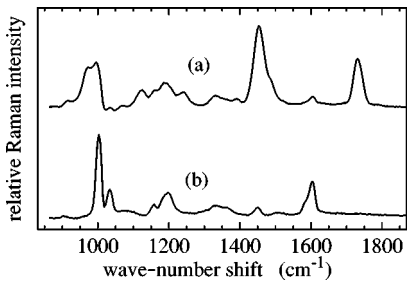

FIG. 5. Raman spectra from the bilayer: (a) spectrum at the $m=1$ mode ($\theta=57.0486°$) in layer $j=3$. PMMA-A contributions are dominant with observable PS-T features at 1004 and 1600 cm^{-1}; (b) spectrum at the $m=1$ mode ($\theta=63.0028°$) for layer $j=2$. PS-T contributions are dominant with no visible evidence of PMMA-A.

depending on θ. Typical spectra, obtained at the $m=1$ condition for the PMMA ($j=3$, curve *a*) and PS ($j=2$, curve *b*) layers are shown in Fig. 5. Separate vibrational features associated with $\overline{\nu}=1600$ cm^{-1} and 1730 cm^{-1} allowed us to concentrate on the source distribution of either polystyrene-toluene (PS-T) or PMMA-acetone (PMMA-A), respectively. The VAIRRS results, $I(\theta|\overline{\nu})$, for these two spectral ranges are shown in Fig. 6.

The waveguide resonances are evident. The two films are optically coupled, leading to a complex interaction. For example, using $\overline{\nu}=1600$ cm^{-1} (which preferentially samples the $j=2$ layer) some enhancement is observed near 57°, where modes within the $j=3$ layer are excited.

These data were simultaneously modeled using Eq. (4) over the seven-dimensional reduced chi-square error spaces $\{n(2),\ h(2),\ n(3),\ h(3),\ C(2|1600),\ C(3|1600),\ \chi^2(1600)\}$ and $\{n(2),\ h(2),\ n(3),\ h(3),\ C(2|1730),\ C(3|1730),\ \chi^2(1730)\}$. The results determined the thickness of the entire structure, 3045 ± 3 nm, and the precise location of the PS/PMMA interface, $z_2=1019\pm2$ nm. In addition, the indices of refraction were found to be $n(2)=1.5955\pm0.0001$, and $n(3)=1.4932\pm(<0.0001)$. The experiment measures the average position of the interface. This does not necessarily mean that the boundary is flat.

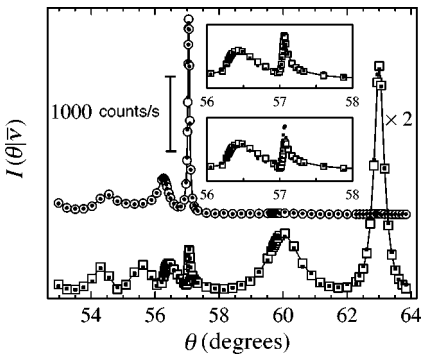

FIG. 6. Bilayer sample: VAIRRS for (squares) the $\overline{\nu}=1600$ cm^{-1} (PS-T) band, and (circles) $\overline{\nu}=1730$ cm^{-1} (PMMA-A) band. The small, solid symbols are the data, the larger, connected symbols show the model. Inset: magnified portion of $I(\theta|1600)$ with $C(3|1600)=0$ (bottom window), and $C(3|1600)=0.0125$ (top window). The implication is that toluene has migrated from the PS (layer 2).

The best fit between the model and the data was achieved with source distributions of $C(2|1600)\equiv 1$, $C(2|1730) = 0.000(+0.025)$, $C(3|1600) = 0.0125 \pm 0.0021$, and $C(3|1730)\equiv 1$. If $C(3|1600)$ was set to zero, rather than 0.0125, the minimum reduced chi-square error increased by 400%. Sensitivity to $C(3|1600)$ was particularly pronounced in $I(\theta|1600)$ in the vicinity of $57°$, shown in the insets of Fig. 6. In a similar manner, the fit was poor using models involving values of $C(2|1730)$ other than 0.000.

The nonzero contribution of the $\overline{\nu} = 1600\ \mathrm{cm}^{-1}$ band in layer $j=3$ suggests that toluene has migrated across the interface, from the PS to the PMMA. This is the only reasonable possibility. The polymers would not have intermixed, since PS and PMMA are immiscible and the annealing steps were conducted well below the glass transition temperatures for either material.

In summary, we have developed a versatile technique (variable angle internal reflection Raman spectroscopy, VAIRRS) for controlling and modeling the optical field distribution in polymer (or other transparent) thin-film systems. We have shown how the method can be used to nondestructively and precisely resolve the spatial distribution of the Raman source function. In an explicit demonstration, we have localized a buried interface between two polymers with a precision of ± 2 nm, and have identified evidence for toluene diffusion from PS into PMMA.

[1] M. Yanagimachi, M. Toriumi, and H. Masuhara, Appl. Spectrosc. **46**, 832 (1992).

[2] R. Iwamoto, M. Miya, K. Ohta, and S. Mima, J. Chem. Phys. **74**, 4780 (1981); R. Iwamoto, K. Ohta, M. Miya, and S. Mima, Appl. Spectrosc. **35**, 584 (1981).

[3] N. H. Fontaine and T. E. Furtak, J. Opt. Soc. Am. B **14**, 3342 (1997).

[4] M. Born and E. Wolf, *Principles of Optics*, 6th ed. (Pergamon Press, Elmsford, New York, 1980), Chap. 1.

[5] The expressions for the integrated intensity given by Yanagimachi *et al.*,[1] are approximate for $\theta < \theta_{c,j}$ and $\theta \gtrsim \theta_{c,j}$. They neglected to properly account for a cross term in the coversion of optical fields to energy density.

[6] This is in agreement with linearly interpolated values from A. C. DeFranzo and B. G. Pazol, Appl. Opt. **32**, 2224 (1993).

[7] Calculated for an altitude of 5280 feet. *American Institute of Physics Handbook*, 3rd ed. (McGraw-Hill, New York, 1972) pp. 6–111.

[8] J. Kressler, N. Higashida, T. Inoue, W. Heckmann, and F. Seitz, Macromolecules **26**, 2090 (1993).

[9] N. Ashby and S. C. Miller, J. Opt. Soc. Am. **67**, 448 (1977).

[10] A. B. Buckman, *Guided-Wave Photonics* (Saunders, Orlando, FL, 1992).

[11] D. R. Miller and P. W. Bohn, Appl. Opt. **27**, 2561 (1988).